Macromolecules

pubs.acs.org/Macromolecules Article

Synthesis of Amphiphilic and Double Hydrophilic Star-like Block Copolymers and the Dual pH-Responsiveness of Unimolecular Micelle

Yeu-Wei Harn, Yanjie He, Zewei Wang, Yihuang Chen, Shuang Liang, Zili Li, Qiong Li, Lei Zhu, and Zhiqun Lin*

Cite This: *Macromolecules* 2020, 53, 8286–8295 Read Online

ACCESS | Metrics & More | Article Recommendations | Supporting Information

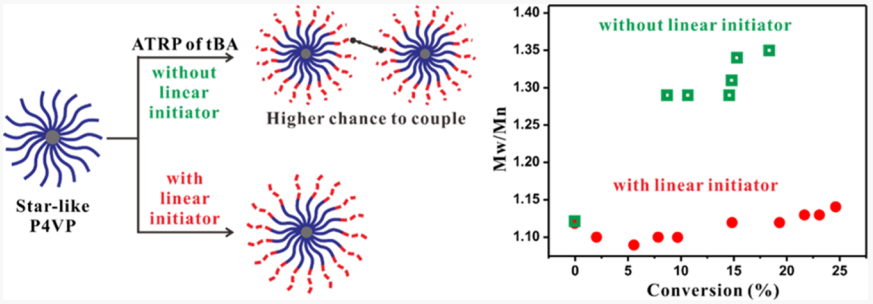

ABSTRACT: A series of amphiphilic star-like triblock copolymers with well-defined molecular architectures, molecular weight, and narrow polydispersity were successfully synthesized by sequential atom transfer radical polymerization (ATRP) using β-cyclodextrin as the initiator. These star-like triblock copolymers are composed of poly(4-vinyl pyridine) (P4VP) as the first block, poly(*tert*-butyl acrylate) (P*t*BA) as the second block, and either polystyrene (PS), poly(methyl methacrylate) (PMMA), or poly(ethylene oxide) (PEO) as the third block (denoted as P4VP-*b*-P*t*BA-*b*-PS, P4VP-*b*-P*t*BA-*b*-PMMA, and P4VP-*b*-P*t*BA-*b*-PEO, respectively). Notably, by deliberate addition of a linear initiator [i.e., ethyl α-bromoisobutyrate (EBiB)] into the polymerization reaction when growing the second P*t*BA block (i.e., synthesis of star-like P4VP-*block*-P*t*BA; denoted as P4VP-*b*-P*t*BA), a suitable concentration of Cu^{2+} can be achieved. This suppresses further termination reactions between active chain ends of star-like polymer, thus rendering the ability to better control the growth of star-like P4VP-*b*-P*t*BA diblock copolymer (polydispersity index; PDI < 1.2). Kinetic studies of P*t*BA polymerization with and without the addition of linear initiators of EBiB were conducted. Importantly, the living nature of ATRP of star-like P4VP-*b*-P*t*BA diblock copolymer can only be attained when the linear initiator was added. Subsequently, star-like P4VP-*b*-P*t*BA-*b*-PS, P4VP-*b*-P*t*BA-*b*-PMMA, and P4VP-*b*-P*t*BA-*b*-PEO were synthesized by using star-like P4VP-*b*-P*t*BA as the macroinitiator via ATRP (for hydrophobic PS and PMMA) and click reaction (for hydrophilic PEO), respectively, further confirming the tunability of surface chemistry (i.e., the outer block of star-like triblock copolymers) in this system. Finally, after hydrolyzing P*t*BA into poly(acrylic acid) (PAA), the dual pH-responsive behaviors of double hydrophilic star-like P4VP-*b*-PAA diblock copolymer were explored. In addition to dual pH-responsiveness, the strategy we developed based on sequential ATRP via cyclodextrin as the initiator in this study may conveniently enable the synthesis of a rich variety of other stimuli-responsive unimolecular star-like block copolymers comprising dissimilar blocks that are either pH-responsive, thermo-responsive, or photo-responsive. As such, they may afford a unique platform for fundamental research and applications in smart delivery vehicles, sensors, and tunable templates for nanomaterials.

INTRODUCTION

The past several decades have witnessed significant advances in the synthesis of polymers with tailorable compositions, structures, and functionalities.[1] Among them, a rich diversity of polymers with nonlinear molecular architectures (e.g., cyclic,[2] dendritic, brush,[3] star-like,[4,5] and hyperbranched[6]) have been extensively studied due to their unique physicochemical,[7] mechanical,[8] photonic,[9,10] and electrical[11] properties for potential applications in molecular recognition,[12] catalysis,[13] drug delivery,[14] and so forth. Star-like polymer represents one of the simplest nonlinear polymers, containing multiple linear arms covalently linked to a core. In general, the method for synthesizing star polymers can be categorized into two

Received: April 21, 2020
Revised: August 10, 2020
Published: September 25, 2020

https://dx.doi.org/10.1021/acs.macromol.0c00918
Macromolecules 2020, 53, 8286–8295

strategies, namely, the "core-first"[3,5,15] and "arm-first"[16] methods. The former strategy uses presynthesized multifunctional initiator as a core, from which subsequent polymerization of monomers produces the multi-arms. On the other hand, the latter involves the preparation of linear arms first, followed by grafting them onto the multifunctional coupling agent, yielding star-like polymers. Clearly, the "core-first" approach provides a better control over the architecture of star-like polymer as the number of arms can be easily tailored by the number of initiate sites of initiators, whereas the "arm-first" route often results in a broad distribution of the number of arms per star-like polymer. Controlled radical polymerizations (CRP), including atom transfer radical polymerization (ATRP) and reversible addition fragmentation chain transfer polymerization, have been proven to be robust techniques for synthesizing well-defined star-like polymers due to their site-specific initiation as well as efficient reversible deactivation. In addition to various initiators as the core, a variety of monomers[17] can be utilized for growing polymeric arms with CRP.

It is widely recognized that synthesizing pyridine-containing polymer with controlled molecular weight (MW) distribution via ATRP remains challenging, especially with increased initiating sites per core, for the following reasons. First, the pyridine group can strongly coordinate with the metal catalysts in the systems, leading to possible formation of pyridine-coordinated metal complexes, which are verified to be non-effective catalysts for the ATRP reaction, thereby greatly reducing the polymerization rate or even rendering uncontrollable polymerization. Second, owing to the ability of halogen atom (especially Br) as the leaving group to nucleophilically attack the pyridyl moiety of pyridine-containing polymers, a significant amount of termination and coupling reactions (i.e., between two star-like polymers as well as polymer arms within a star-like polymer) and thus a sharp increase in polydispersity occurs. Furthermore, this phenomenon would become more severe when the number of initiating sites per core increases because of higher tendency of arm−arm coupling within one star-like polymer due to the closer proximity between initiating sites.[18,19] In addition, the synthesis of star-like diblock or triblock copolymers by ATRP with the pyridine-containing polymer as the first block has been comparatively less and limited in scope as the issues noted above remain for the subsequent polymerization of the second or the third block.

On the other hand, stimuli-responsive polymers represent an intriguing class of materials as their physical and chemical properties can be conveniently tuned upon exposure to external stimuli (e.g., temperature, pH, and electric fields).[9,20] Among them, poly(4-vinylpyridine) (P4VP) has been extensively studied owing to its good pH-sensitivity, biocompatibility, and hydrophilicity.[21,22] Notably, P4VP has often been exploited as a drug carrier due to its enhanced solubility (i.e., fully stretched P4VP chain) under a lower pH value, resulting in the release of drug locally (e.g., in the acid environment of tumors).

Herein, we report a route to synthesize a set of star-like homopolymer, diblock and triblock copolymer, containing P4VP as the first block, with low polydispersity by the addition of a linear initiator [ethyl α-bromoisobutyrate (EBiB)], followed by investigating the dual pH-responsive behavior of star-like poly(4-vinyl pyridine)-*block*-poly(acrylic acid) (P4VP-*b*-PAA) diblock copolymer. The star-like triblock copolymers comprise P4VP as the first block, poly(*tert*-butyl acrylate) (P*t*BA) as the second block, and either polystyrene (PS), poly(methyl methacrylate) (PMMA), or poly(ethylene oxide) (PEO) as the third block (denoted as P4VP-*b*-P*t*BA-*b*-PS, P4VP-*b*-P*t*BA-*b*-PMMA, and P4VP-*b*-P*t*BA-*b*-PEO, respectively). Specifically, the initiator for ATRP with 21 initiating sites is first formed via bromination of β-cyclodextrin. After successful synthesis of the first P4VP block with tailorable MW and narrow polydispersity, star-like P4VP-*block*-poly(*tert*-butyl acrylate) (P4VP-*b*-P*t*BA) diblock copolymers with controlled MW distribution can be prepared by deliberate addition of an optimal amount of linear initiators of EBiB to prevent the coupling reaction between two star-like polymers as well as polymer arms within a star-like polymer. When the molar ratio between initiate sites [including sites from both star-like P4VP homopolymer terminated with X (X = Cl and Br) and linear initiators of EBiB] and metal catalysts of CuCl is increased to 1 to 1, suppressed tendency of the coupling between the arms of star-like diblock copolymer as well as between adjacent star-like diblock copolymers and thus narrow polydispersity is achieved. The polymerization kinetics of the second P*t*BA block with and without the addition of linear initiators of EBiB is scrutinized. The linear relationship of $\ln([M]_0/[M])$ ($[M]_0$ and $[M]$ are the monomer concentrations at t_0 and t, respectively) versus time can only be attained when the linear initiator of EBiB is present, indicating that the number of propagating species remains constant during polymerization. As a result, this synthetic approach can facilitate the preparation of multi-arm polymers, specifically consisting of the pyridine-containing polymer as the first block, with controlled MW distribution (i.e., generally below 1.2). Moreover, as-synthesized star-like P4VP-*b*-P*t*BA diblock copolymer terminated with X (X = Cl and Br) could continue serving as a macroinitiator for the third polymerization, yielding star-like triblock copolymers. Successful synthesis of star-like P4VP-*b*-P*t*BA-*b*-PS and P4VP-*b*-P*t*BA-*b*-PMMA triblock copolymers by ATRP as well as P4VP-*b*-P*t*BA-*b*-PEO by the click reaction demonstrates the versatility of this synthetic strategy. Furthermore, the dual pH change-induced responsive behavior of star-like P4VP-*b*-PAA diblock copolymer obtained via thermolysis of P*t*BA of star-like P4VP-*b*-P*t*BA into PAA is examined via dynamic light scattering (DLS) and UV−vis studies under various pH environments, and the possible morphological change is proposed. Taken together, the results suggest the promising potential of the as-synthesized star-like diblock copolymer as polymeric nanocarriers for controlled release of drugs.

RESULTS AND DISCUSSION

Synthesis of Initiator with 21 Initiating Sites for Subsequent ATRP Reactions. A facile synthesis approach based on the previous literature[5,23] to modify the end hydroxyl groups of β-cyclodextrin (β-CD) by capitalizing on 2-bromoisobutyl bromide was conducted. After mixing β-CD with an esterification agent (i.e., α-bromoisobutyryl bromide) for one day under room temperature, the outer hydroxyl groups can be substituted by the bromoisobutyryl units, yielding 21-Br-β-CD (left panel in Scheme 1a). 1-Methyl-2-pyrrolidone (NMP) was identified as a suitable solvent for esterification due to its compatibility with the esterification agent and a small amount of HBr byproduct. The successful esterification of β-CD was corroborated by proton nuclear magnetic resonance (^{1}H NMR) (Figure S1), where the methyl protons of 21-Br-β-CD (assigned to δ = 1.8−2.2) were seen. The conversion efficiency of the end hydroxyl group can be calculated by the equation

$$E_T = \frac{A_b}{18A_a} \times 100\%$$

https://dx.doi.org/10.1021/acs.macromol.0c00918
Macromolecules 2020, 53, 8286−8295

Scheme 1. (a) Schematic Illustration of the Synthetic Route to Star-like P4VP-*b*-P*t*BA Diblock Copolymer (1) Without and (2) With the Addition of Linear Initiators of EBiB, Where BMP Is 2-Bromo-2-methylpropionate. (b) Schematic Representation of Synthetic Strategies for (1) Star-like P4VP-*b*-PAA Diblock Copolymer via Hydrolysis of Inner P*t*BA Block, (2 and 3) Star-like P4VP-*b*-P*t*BA-*b*-PS and P4VP-*b*-P*t*BA-*b*-PMMA Triblock Copolymers by Using Star-like P4VP-*b*-P*t*BA Diblock Copolymer as Macroinitiator for ATRP of Styrene and Methyl Methacrylate, Respectively, and (4) P4VP-*b*-P*t*BA-*b*-PEO via Click Reaction of Star-like P4VP-*b*-P*t*BA and Linear PEO

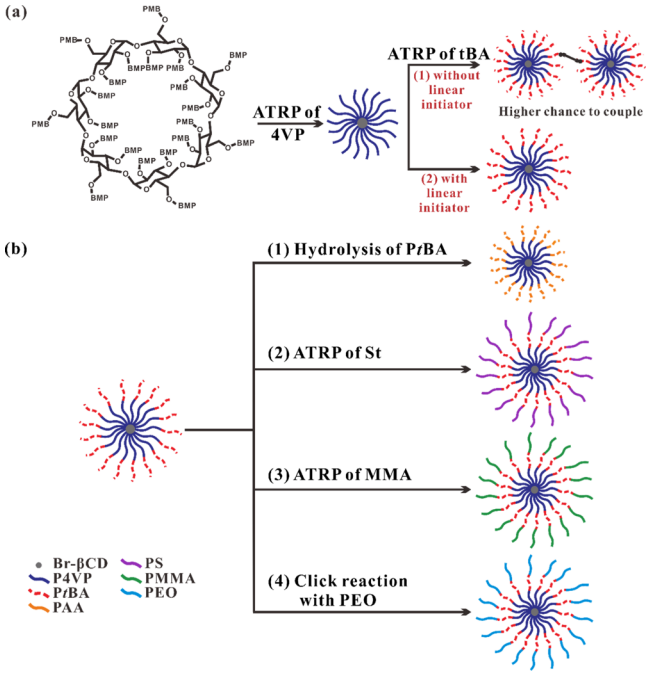

where E_T is the conversion efficiency of hydroxyl groups, and A_a (δ = 5.2−5.3) and A_b are the integral areas of the part of the residual protons on β-CD and the methyl protons, respectively. Based on the calculation, as-synthesized 21-Br-β-CD showed a conversion as high as 95%, indicating the successful substitution of hydroxyl groups into bromoisobutyryl units, yielding the initiator for the subsequent ATRP.

Synthesis of Star-like P4VP Homopolymer via the First ATRP. By using the 21-Br-β-CD as the initiator and CuCl/Me_6TREN as the cocatalyst (see Experimental Section in the Supporting Information), ATRP of 4-vinyl pyridine (4VP) was successfully conducted in 2-propanol at 40 °C. As reported in the literature, polymerization of 4VP via ATRP can be difficult due mainly to (1) the coordination between metal catalysts (i.e., CuCl) and pyridyl groups of 4VP/P4VP in the system and (2) the coupling between the halide group at polymer chain end of each star-like polymer and the pyridyl group of 4VP and P4VP,[24] both resulting in the occurrence of termination and/or coupling reaction, and thus broadened the MW distribution. In order to obtain star-like P4VP with tailorable MW and controlled polydispersity, several experimental parameters were tailored. First, instead of CuBr/PMDETA, CuCl/Me_6TREN were used as cocatalysts. It is notable that CuCl was chosen as the metal catalyst because of the weak ability of chlorine atom as the leaving group, thereby resulting in less susceptibility to nucleophilically attack pyridyl groups of P4VP and thus reduced side reactions in the system. In sharp contrast, a significant termination reaction can be observed, represented by the appearance of the shoulder peak or broad polydispersity from gel permeation chromatography (GPC) result, when CuBr was used as the metal catalyst for polymerizing 4VP via ATRP. Furthermore, due to the lower activation/deactivation equilibrium constant of alkyl chloride, Me_6TREN was selected as the ligand to increase polymerization speed. Moreover, the strong coordination between CuCl and Me_6TREN ligands can facilitate the removal of the catalyst by passing the polymer solution through an alumina column or directly stirring alumina in the product solution, as verified by color change from green to colorless or pale yellow after the abovementioned treatments. In addition to changing cocatalysts (i.e., CuCl and Me_6TREN), reducing reaction temperature and reaction time were found to be helpful for suppressing the occurrence of the coupling reaction.

Three star-like P4VP homopolymers with different MWs and narrow MW distribution (typically lower than 1.1) were synthesized. Monomodal peaks can be observed from the GPC results (Figures 1 and S2), and the MW can be easily tuned

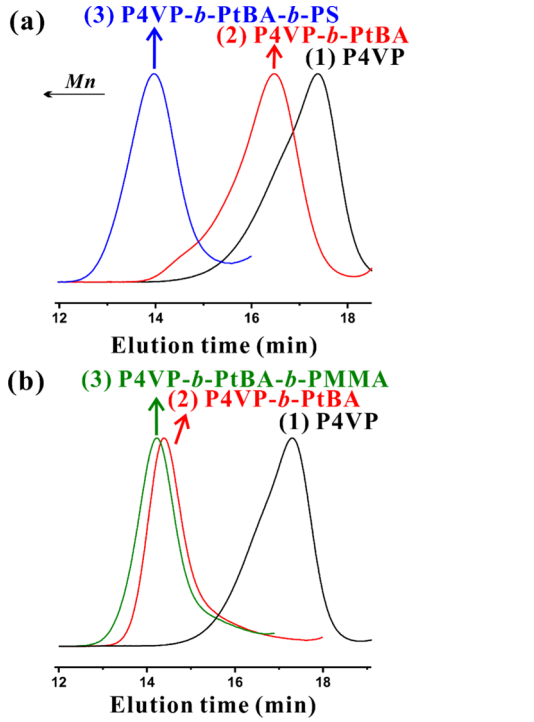

Figure 1. (a) GPC traces of (1) star-like P4VP homopolymer, (2) P4VP-*b*-P*t*BA diblock copolymer, and (3) P4VP-*b*-P*t*BA-*b*-PS triblock copolymer. (b) GPC traces of (1) star-like P4VP homopolymer, (2) P4VP-*b*-P*t*BA diblock copolymer, and (3) P4VP-*b*-P*t*BA-*b*-PMMA triblock copolymer.

by changing the polymerization time. The MWs of all the as-synthesized star-like polymers are summarized in Table S1. Notably, low polydispersity index (PDI) and no obvious shoulder peak appeared in the high MW range, indicating that there were no intermacromolecular coupling reactions. Very little linear P4VP homopolymer appeared, suggesting the suitable condition chosen for ATRP of 4VP with star-like Br-β-CD as the initiator. Representative ^{1}H NMR spectrum of star-like P4VP homopolymer obtained after reacting for 6 h is shown in Figure 2a. The characteristic chemical shifts of ^{1}H NMR at δ =

https://dx.doi.org/10.1021/acs.macromol.0c00918
Macromolecules 2020, 53, 8286−8295

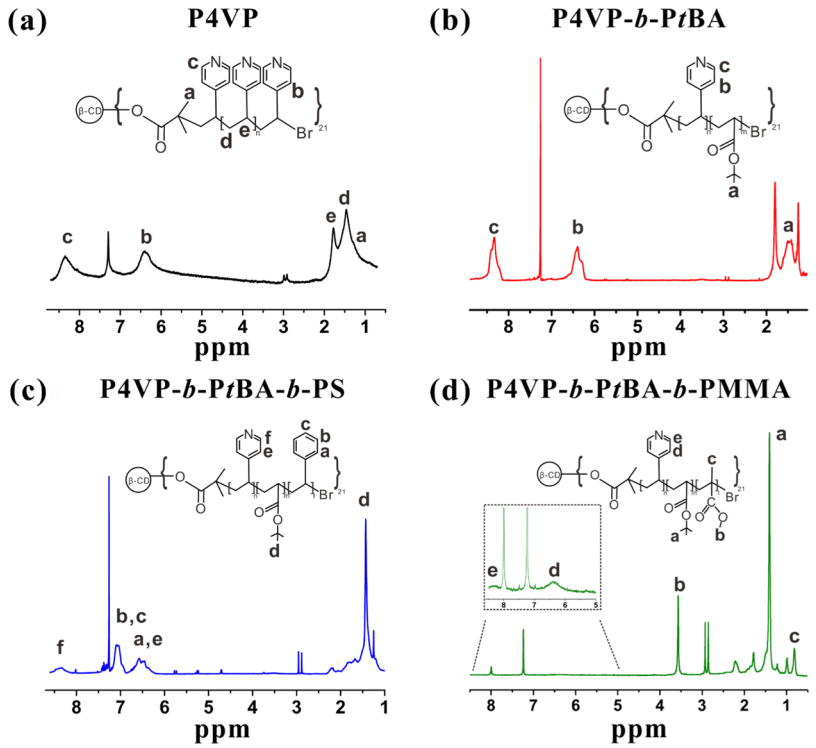

Figure 2. ^{1}H NMR spectra for (a) star-like P4VP homopolymer, (b) star-like P4VP-*b*-P*t*BA diblock copolymer, (c) star-like P4VP-*b*-P*t*BA-*b*-PS triblock copolymer, and (d) star-like P4VP-*b*-P*t*BA-*b*-PMMA triblock copolymer. All samples are measured in $CDCl_3$.

6.6 (marked as b in Figure 2a) and δ = 8.3 (marked as c in Figure 2a) corresponded to the protons of the pyridyl group, indicating successful synthesis of P4VP block.

Synthesis of Star-like P4VP-*b*-P*t*BA Diblock Copolymers with Low Polydispersity via the Second ATRP. A series of star-like P4VP-*b*-P*t*BA diblock copolymers with different MWs and controlled PDI were subsequently synthesized via ATRP using the as-synthesized star-like P4VP homopolymer as the macroinitiator (central panel in Scheme 1a). The effect of addition of a linear initiator of EBiB on MW distribution was scrutinized. This was motivated by the observation of broad peak and/or shoulder in GPC traces during the synthesis of the second star-like P*t*BA block. Notably, we tried to reduce the influence of partially oxidized metal catalyst (i.e., CuCl; it has been difficult to estimate the extent of oxidation as it varied as time went by, even stored the metal catalysts inside the glovebox) by keeping the metal catalyst amount no less than 10 mg at each ATRP. A small amount of attainable star-like P4VP block and constant amount of metal catalyst (typically ~10 mg) resulted in a low ratio of initiator to the metal catalyst. We thus speculate that the irregular peak shape of GPC traces may be due to the synergic effect of the use of highly active ligand,[25] small molar ratio (i.e., 0.02) of the initiation sites from star-like P4VP homopolymer to the metal catalyst, and the architecture of star-like polymer (i.e., closer distance between the radical within one star-like polymer), thereby generating radicals (i.e., active species during ATRP) with higher concentrations and increasing the occurrence of termination and/or coupling reactions, which is often seen in surface-initiated living radical polymerization.[26,27] Based on the solutions reported previously with surface-initiated polymerization, we deliberately added the predetermined amount of a linear initiator of EBiB with a 1:1 molar ratio of EBiB to the metal catalyst to the reaction mixture. Consequently, the addition of the linear initiator rendered an appropriate ratio of initiator sites (i.e., halide groups from both star-like P4VP-*b*-P*t*BA diblock copolymers and linear EBiB initiators) to the metal catalyst CuCl. Thus, the concentration of Cu^{2+} was increased, ensuring a fast deactivation process and suppressing further termination reactions from radical coupling (see equation below) in the system and leading to better control over the chain growth of the star-like diblock copolymer.

$$P{-}X + Cu^{I}Cl/Me_6TREN \leftrightarrow P^{*} + Cu^{II}Cl_2/Me_6TREN$$

As a result, by employing the strategy described above, star-like P4VP-*b*-P*t*BA diblock copolymers with monomodal GPC traces were obtained (Figure S3), and the MW of the resulting star-like P4VP-*b*-P*t*BA can be readily controlled by tuning the reaction time. Figure 2b shows the ^{1}H NMR spectrum of the as-obtained star-like P4VP-*b*-P*t*BA diblock copolymer. The appearance of the strong characteristic peak at δ = 1.45 (marked as a in Figure 2b), corresponding to the methyl protons in the *tert*-butyl group [$-C(CH_3)_3$], confirmed the success in growing P*t*BA onto star-like P4VP block.

The polymerization kinetics with and without the addition of linear initiators of EBiB were then studied (Tables S2 and S3). Figure 3a displays a linear relationship of semilogarithmic kinetic plot when the linear initiator was added, suggesting the radical concentration was constant during polymerization. Conversely, a nonlinearity was seen in the absence of the linear initiator, signifying possible occurrence of termination and/or coupling reactions due to the competing side reactions, that is, termination reactions from the radical (i.e., active species within ATRP) coupling and/or coupling between halide groups of star-like polymer chain end and pyridyl groups within the first star-like P4VP block. Clearly, the addition of a linear initiator was thus proven to be effective in reducing the side reaction by decreasing the concentration of active species in the ATRP

https://dx.doi.org/10.1021/acs.macromol.0c00918
Macromolecules 2020, 53, 8286−8295

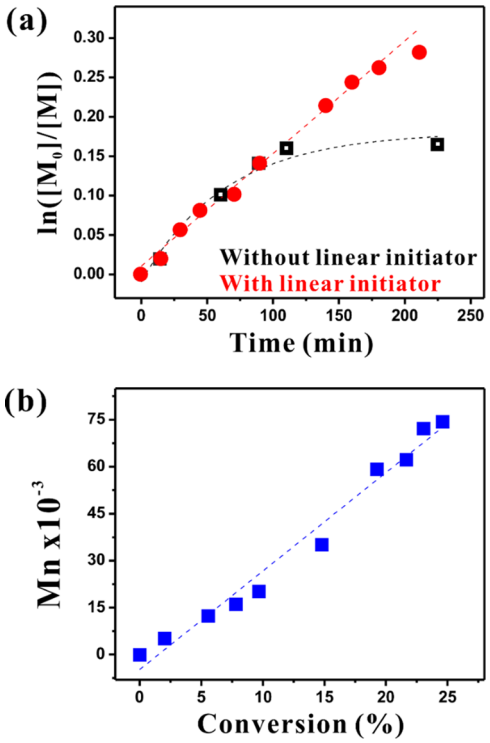

Figure 3. (a) Kinetic plot for the copper-mediated ATRP of the second P*t*BA block with and without the addition of linear initiators of EBiB, employing star-like P4VP homopolymers as the macroinitiator and dimethylformamide (DMF) as the reaction solvent. $[M_0]$ and $[M]$ are the concentration of the *t*BA monomer at time 0 and *t*, respectively. (b) Dependence of number average MW (M_n) of the second P*t*BA block on the *t*BA monomer conversion.

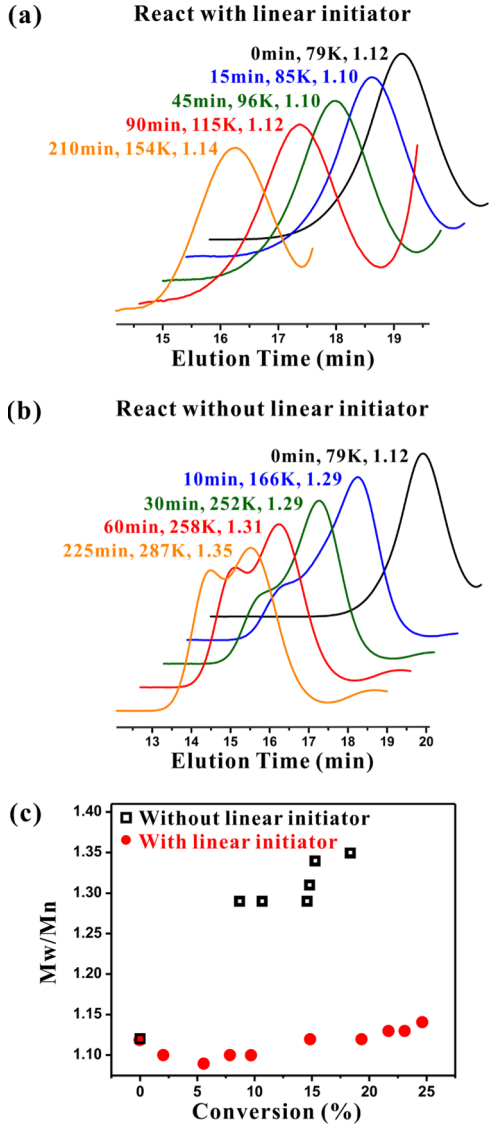

Figure 4. GPC chromatograms of star-like P4VP-*b*-P*t*BA diblock copolymers prepared by ATRP (a) with and (b) without the addition of linear initiators of EBiB. Three numbers marked next to each curve refer to the reaction time, M_n, and PDI (M_w/M_n), respectively. (c) Dependence of M_w/M_n for star-like P4VP-*b*-P*t*BA diblock copolymers on *t*BA monomer conversion.

system. A linear increase of number average MW (M_n) of the second P*t*BA block versus *t*BA monomer conversion was identified when growing the second P*t*BA block with the presence of EBiB (Figure 3b). Both linear kinetic plots of $\ln([M]_0/[M])$ versus time and linear relationship between M_n and monomer conversion corroborated that the successful polymerization of the second P*t*BA block, using the first star-like P4VP block as the macroinitiator with addition of a linear initiator, is controlled/living radical polymerization with a negligible amount of transfer and termination reactions. Furthermore, the PDI can be significantly suppressed with the presence of a linear initiator (as shown in Figure 4). The PDI remained lower than 1.15 after polymerization for 210 min with the addition of EBiB, while it increased to 1.35 with a similar reaction time in the absence of EBiB. With no EBiB in the system, the shoulder peak started to appear due to the intra- and intermolecular coupling reaction even with only 10 min polymerization time, and the PDI continued increasing with the prolonged reaction time. Figure 4c compares the PDI when growing the second P*t*BA block from the star-like P4VP homopolymer in the presence and absence of linear initiators of EBiB.

On the basis of the results described above, by employing the additional linear initiator, its effect in suppressing the occurrence of coupling and/or termination reactions, resulting from increasing concentrations of Cu^{2+}, and in turn, a faster deactivation process can thus be substantiated. Furthermore, this approach by judiciously introducing the linear initiator is particularly beneficial when synthesizing star-like, pyridine-containing polymers due to closer proximity between radicals within each star-like polymer and using more active ligand (i.e., Me_6TREN). The addition of linear initiators can thus lead to markedly improved controllability of the growth of polymer chains (i.e., narrow polydispersity).

Moreover, the appropriate amount of the linear initiator (EBiB) added was also investigated. Figure S4 compares the GPC traces of the growth of the second P*t*BA block with various amounts of linear initiators added yet with the same reaction time. The optimal amount was found when the ratio of linear initiator to metal catalyst (CuCl) is 1 to 1 (central panel; Figure S4). At a low amount of a linear initiator (i.e., molar ratio of EBiB/CuCl is 0.5 to 1), the peak still broadened with increased PDI (upper panel; Figure S4). The peak broadening became even more obvious with a prolonged polymerization time (Figure S5). On the other hand, with an excess amount of EBiB added (i.e., molar ratio of EBiB/CuCl is 1 to 1.5), the polymerization speed decreased (lower panel; Figure S4)

https://dx.doi.org/10.1021/acs.macromol.0c00918
Macromolecules 2020, 53, 8286−8295

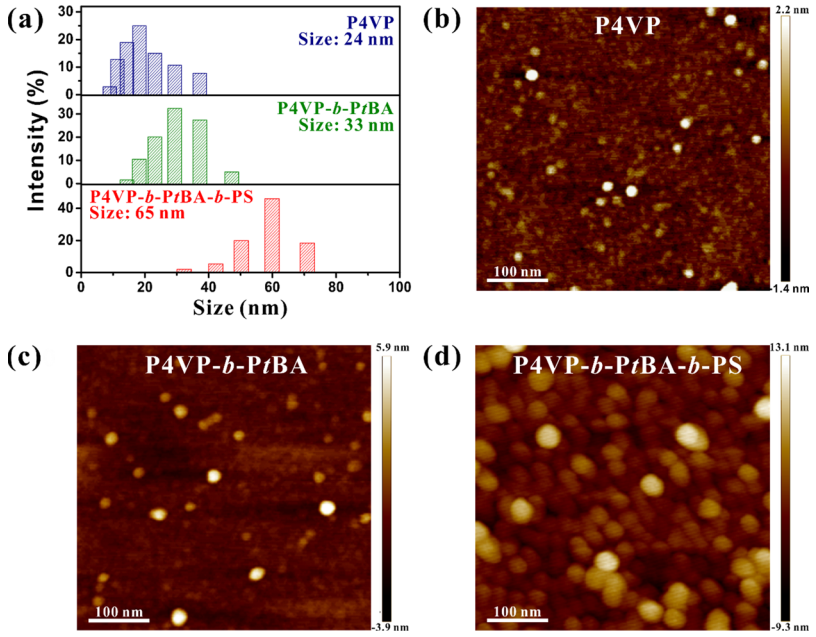

Figure 5. (a) Size change from star-like P4VP homopolymer, P4VP-*b*-P*t*BA diblock copolymer to P4VP-*b*-P*t*BA-*b*-PS triblock copolymer at 25 °C, as measured by DLS. (b–d) AFM height images of the corresponding star-like (b) P4VP homopolymer, (c) P4VP-*b*-P*t*BA diblock copolymer, and (d) P4VP-*b*-P*t*BA-*b*-PS triblock copolymer. Image size = 0.5 μm × 0.5 μm.

possibly because both star-like P4VP and linear initiators competed for reacting with *t*BA monomers.

We note that another possibility to reduce the polymerization speed for better control over PDI is to introduce additional $CuCl_2$, as reported in the literature. To this end, $CuCl_2$ with varied amounts (i.e., the molar ratios of $CuCl_2$ to CuCl are 0, 0.27, and 0.54) was added to elucidate the effect of $CuCl_2$ on polymerization. From the GPC traces, as shown in Figure S6, broad peak can be observed in all cases regardless of the amount of $CuCl_2$ added. This may be because even with the presence of $CuCl_2$ (especially within the range tried), the ratio between metal catalysts to initiating sites of star-like P4VP homopolymers may still remain high, suggesting that the approach to decrease coupling and/or termination reactions via adding $CuCl_2$ was not effective in this system.

Initially, the polymerization of the second P*t*BA block was carried out with an $[M]_0/[I]_0$ ratio of 520, as shown in Table S2, where $[M]_0$ and $[I]_0$ are the initial concentrations of monomer and overall initiation sites from both star-like P4VP and linear initiators. Star-like P4VP-*b*-P*t*BA diblock copolymers with narrow MW distribution can be synthesized with monomer conversion up to 25% after 3–4 h. When conversion was larger than 25–30%, the polymerization speed gradually decreased with the prolonged reaction time (Figure S7), due possibly to unavoidable termination reactions, loss of catalyst activity, and/or increasing steric hindrance around the reactive chain ends.[28] However, low conversion was reported to be beneficial for acquiring non-linear polymer with the well-controlled structure (e.g., narrow PDI) by suppressing undesirable side reactions.[29] Moreover, we found that by raising the molar ratio of $[M]_0/[I]_0$ from 520 to 780, the MW of the second P*t*BA block can be further increased. The MW of P*t*BA block was enlarged when the *t*BA monomer amount was increased while keeping other experimental conditions the same. The GPC traces of ATRP of the second P*t*BA block with different amounts of monomers are shown in Figure S8. Compared to employing the ratio of 520 at a specific reaction time (marked as a-1 and a-2 in Figure S8, respectively), P*t*BA with larger MW can be acquired when the ratio increased to 780 (marked as b-1 and b-2 in Figure S8) at both reaction times. Remarkably, the PDI can still be maintained less than 1.2. The MW of the second P*t*BA block can thus be increased simply by increasing the *t*BA monomer amount even with the monomer conversion still lower than 30%.

Despite good controllability in PDI by adding the linear initiator during the reaction, the appearance of the linear P*t*BA block was inevitable. Typically, fractional precipitation can be utilized to remove the undesired linear polymer, that is, by the fact that the polymer with larger MW would precipitate out first when dissolving the polymer in good solvent with the gradual addition of poor solvent. In this case, the difficulty of conducting fractional precipitation lies in identifying good solvent and poor solvent for both P4VP and P*t*BA blocks at the same time. Intriguingly, we found that the linear P*t*BA can be easily removed by washing the product with hexane (Figure S9). Employing the solubility difference of P4VP and P*t*BA in hexane (good solubility for P*t*BA and poor solubility for P4VP), linear P*t*BA is soluble in hexane whereas star-like P4VP-*b*-P*t*BA diblock copolymers cannot be well dissolved in hexane, resulting in easy separation of the two parts via washing the product, followed by centrifuging and collecting the precipitant. Notably, the larger the MW of the outer P*t*BA block, the higher tendency for dissolving the star-like diblock copolymer in hexane at the same time, eventually leading to more losses during this washing process.

Synthesis of Star-like P4VP-*b*-P*t*BA-*b*-PS and P4VP-*b*-P*t*BA-*b*-PMMA Triblock Copolymers via the Third ATRP. A series of star-like P4VP-*b*-P*t*BA-*b*-PS and P4VP-*b*-P*t*BA-*b*-PMMA triblock copolymers with different MWs were successfully prepared by conducting third ATRP using the star-like P4VP-*b*-P*t*BA diblock copolymer as the macroinitiator (Scheme 1b2,b3, respectively). The absence of intermacromolecular coupling was verified by the GPC traces of star-like P4VP-*b*-P*t*BA-*b*-PS and P4VP-*b*-P*t*BA-*b*-PMMA triblock copolymers (Figures 1 and S10). Figure 2c–d shows the

https://dx.doi.org/10.1021/acs.macromol.0c00918
Macromolecules 2020, 53, 8286–8295

representative ^{1}H NMR spectra of star-like P4VP-*b*-P*t*BA-*b*-PS and P4VP-*b*-P*t*BA-*b*-PMMA triblock copolymers, respectively. As shown in Figure 2c, except for those characteristic chemical shifts from previous blocks, the peaks at δ = 6.33−7.31 can be assigned to the protons on the phenyl ring of the third PS block, indicating the successful growth of PS onto the star-like P4VP-*b*-P*t*BA macroinitiator. On the other hand, the chemical shift shown in Figure 2d at δ = 0.8−1.12 can be ascribed to methyl groups of the third PMMA block. The weak signal at δ = 6.6 and 8.3 from the pyridine group of the first star-like P4VP block might be due to the small ratio of MW between P4VP and the subsequent P*t*BA and PMMA block.

It is notable that when performing ATRP for the second (*t*BA) or third block (styrene and methyl methacrylate, respectively), even though the macroinitiator [e.g., X-terminated (X = Cl and Br) star-like P4VP in the case of grafting second P*t*BA block] was dissolved in good solvent at the beginning, the addition of *t*BA monomers may still cause turbidity or precipitation because *t*BA was the poor solvent for star-like P4VP homopolymers. As a result, the molar ratio of solvent to monomer was an important parameter that we paid attention to and the speed of adding *t*BA monomers should be controlled, that is, a dropwise injection was preferred to prevent the precipitation of the macroinitiator.

To further understand the sizes and morphologies of these structurally stable spherical macromolecules, both DLS and atomic force microscopy (AFM) characterizations were conducted. First, the hydrodynamic diameters D_h of the star-like P4VP homopolymer, star-like P4VP-*b*-P*t*BA diblock copolymer, and star-like P4VP-*b*-P*t*BA-*b*-PS triblock copolymer were measured by DLS (Figure 5a). In particular, all three kinds of star-like polymers were completely dissolved in DMF (c = 1 mg/mL), which is a good solvent for all three polymer blocks, thus resulting in the formation of a unimolecular micelle. Clearly, the D_h of the polymer increased from 24, 33 to 65 nm when an additional block was polymerized, suggesting that each block was successfully grown from the previous star-like initiator. In addition, AFM measurements were conducted to distinguish the structure of unimolecular star-like polymers. A DMF solution (c = 1 mg/mL) containing star-like P4VP, P4VP-*b*-P*t*BA, and P4VP-*b*-P*t*BA-*b*-PS (sample 1; Table S1) was spin-coated on the pre-cleaned Si substrate at the spin speed of 3000 rpm for 30 s, and the results are shown in Figure 5b−d, respectively. The spherical unimolecular nanoparticulates are clearly evident with an average diameter of 19.9 ± 3.4, 29.1 ± 4.5, and 59.7 ± 5.9 nm for the star-like P4VP homopolymer, star-like P4VP-*b*-P*t*BA diblock copolymer, and star-like P4VP-*b*-P*t*BA-*b*-PS triblock copolymer (Figure S11), respectively, correlating well with the D_h results from the DLS measurements.

Synthesis of Star-like P4VP-*b*-P*t*BA-*b*-PEO via Click Reaction. In addition to using ATRP for the growth of the third block of the star-like triblock copolymer, hydrophilic PEO can be grafted onto the star-like P4VP-*b*-P*t*BA diblock copolymer via the click reaction, suggesting the capability of tailoring surface chemistry (i.e., the outer block of the star-like triblock copolymers) in this star-like polymer system. To proceed with the reaction, the halogen end groups (i.e., Cl and Br) on star-like P4VP-*b*-P*t*BA diblock copolymers were first transformed into azide functionalities through nucleophilic substitution reactions with NaN_3 in DMF. Successful azidation can be confirmed by the appearance of the stretching of $-N_3$ at 2112 cm^{-1} in Fourier transform infrared spectroscopy (FTIR) result (Figure S12a, indicated by the black arrow). Subsequently, the click reaction between star-like P4VP-*b*-P*t*BA-N_3 and alkyne-terminated PEO was performed. During the click reaction, excess amount of alkyne-terminated PEO was added into the system to ensure that all the star-like P4VP-*b*-P*t*BA arms were clicked with linear PEO. The unreacted linear alkyne-terminated PEO can be removed facilely by precipitating in cold methanol for several times. The successful click reaction can be verified by GPC traces with a significant peak shift (Figure S12b), signifying the effective grafting of linear PEO onto the star-like P4VP-*b*-P*t*BA diblock copolymer.

Dual pH-Responsive Star-like P4VP-*b*-PAA Diblock Copolymer. Both hydrophilic P4VP and PAA are such weak polyelectrolytes that the degree of ionization is governed by pH and ionic strength of the aqueous solution. At higher pH (basic medium), PAA chains are deprotonated and fully stretched due to the repulsion of negatively charged PAA chains, whereas at lower pH (acid medium), P4VP chains can be fully stretched due to the repulsion of positively charged P4VP chains. Moreover, the strong ionization on either P4VP or PAA block can facilitate the redissolution of the star-like diblock copolymer.[30] Before investigating the pH-responsive behaviors of star-like P4VP-*b*-PAA diblock copolymers, we first looked into the pH-responsive behaviors of star-like P4VP the and star-like PAA homopolymer, respectively. The UV−vis transmittance and DLS results of the star-like P4VP homopolymer (MW from GPC = 75k, blue curve in Figure S2) and the star-like PAA homopolymer (MW from GPC = 290k) under different pH values in aqueous solution were obtained to indirectly characterize the associated morphological change of star-like polymers under different pH environments. Size and transmittance change of star-like P4VP homopolymers under varied pH values are shown in Figure S14. The hydrodynamic diameter of the P4VP remained the same size at pH = 1 and 2, slightly decreased when pH increased to 3, followed by a continuous increase at pH value higher than 5. The size distribution and size change at different pH values are shown in Figure S14a and Figure S14b, respectively. At pH ≤ 2, the star-like P4VP homopolymer was fully dissolved and polymer chains were fully stretched, yielding a transparent solution (Figure S13). With increased pH, the deprotonation of the P4VP side chains and side chain aggregation toward the core occurred, resulting in a slight decrease in the size (at pH = 3). With further increased pH, the dispersed star-like P4VP started to form large intermolecular aggregates, leading to a sharp increase in the size (inset in Figure S14b).

In addition to the pH-dependent size change measured by DLS, the transmittance of solution containing star-like P4VP homopolymers provided further support on the proposed morphological change under different pH environments (Figure S14c). At pH > 2, the solution transmittance gradually decreased, resulting from the deprotonation of P4VP side chains and reduced electrostatic repulsion between star-like P4VP homopolymers. At pH > 3, the transmittance rapidly dropped due to the occurrence of the collapse of the deprotonated side chains and intermolecular aggregation.

On the other hand, the size and transmittance variations of star-like PAA homopolymers under various pH environments were also measured and summarized in Figure S15. Similar to the size change trend of star-like P4VP except that PAA dissolved better at higher pH due to the deprotonated polymer chains, in the star-like PAA homopolymer case, with decreasing pH, the polymer size first slightly reduced with partially collapsed polymer chains, followed by continuous increase in

https://dx.doi.org/10.1021/acs.macromol.0c00918
Macromolecules 2020, 53, 8286−8295

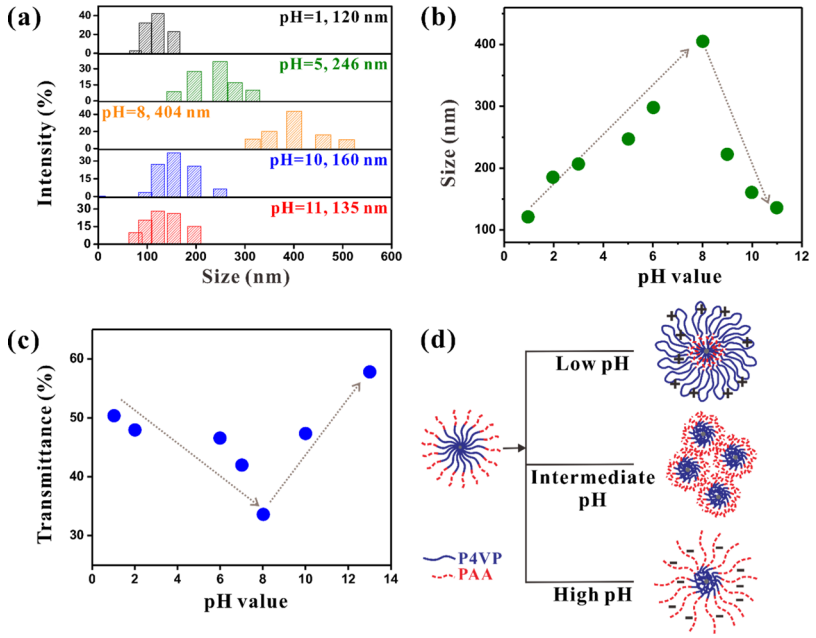

Figure 6. (a) Size change of double hydrophilic star-like P4VP-*b*-PAA diblock copolymer at different pH values at 25 °C, as measured by DLS. (b) Relation between average hydrodynamic diameter of P4VP-*b*-PAA diblock copolymer and pH value, summarized from DLS data in (a). (c) UV−vis transmittance of star-like P4VP-*b*-PAA diblock copolymers at 450 nm as a function of pH. The sample concentration is 1 mg/mL. (d) Proposed morphological changes of star-like P4VP-*b*-PAA under various pH environments.

size because of intermolecular aggregation between star-like PAA homopolymers. Moreover, UV−vis measurement of star-like PAA showed consistent results with the continuous increase in transmittance with increasing pH. Taken together, both star-like P4VP and star-like PAA were thus demonstrated to be pH-responsive with opposite size change under varied pH conditions. Given the pH responses of star-like P4VP and PAA homopolymers, a dual pH response of a star-like P4VP-*b*-PAA diblock copolymer may thus be expected.

To obtain a star-like P4VP-*b*-PAA diblock copolymer, star-like P4VP-*b*-P*t*BA diblock copolymers with narrow PDI (sample 1 without growing third PS block; Table S1) were first dissolved in DMF, followed by raising to refluxing temperature and reacting for 4 h. *tert*-Butyl substituent of P*t*BA block can then be thermolyzed selectively and efficiently, yielding the star-like P4VP-*b*-PAA diblock copolymer for the pH-responsive behavior study. Figure 6 depicts the size (Figure 6a,b) and transmittance changes (Figure 6c) of star-like P4VP-*b*-PAA diblock copolymers under different pH environments. Surprisingly, by monitoring the appearance of the solution under different pH values, we found the solutions were turbid despite being dissolved in acid or basic environments, due possibly to the interference of the insolubility of the other different blocks in the star-like P4VP-*b*-PAA system. For instance, P4VP dissolved well in acid conditions, whereas PAA had low solubility in acid conditions, thus still leading to slight aggregation, as confirmed by only a slight increase in size. Similar behavior was observed in the basic environment. Intriguingly, a continuous size increase from pH = 5 to pH = 8 was found with the most significant increase occurred at pH = 8 (Figure 6b). We speculated that for the pH value in this range, the positively charged pyridine groups and negatively charged carboxyl groups in the star-like P4VP-*b*-PAA diblock copolymer may compensate their opposite charges that diminish the electrostatic repulsion, thereby leading to aggregation between star-like P4VP-*b*-PAA.

The possible mechanism accounting for the size change under different pH values is schematically illustrated in Figure 6d. In the basic environment (i.e., a good solvent for PAA block, yet a poor solvent for P4VP block), the outer deprotonated PAA block could be fully stretched because of the electrostatic repulsion, whereas the inner P4VP block would be collapsed, thus resulting in stabilization of the star-like P4VP-*b*-PAA diblock copolymer to some extent. On the other hand, under acid conditions (i.e., a good solvent for P4VP block, yet a poor solvent for PAA block), the shrunk PAA chains would collapse onto the core, and meanwhile, the P4VP block would extend into the acidic solution, forming the inversed unimolecular micellar structure. This observation is similar to the results from the previous literature.[21,31] Again, due to the electrostatic repulsion between P4VP chains, star-like P4VP-*b*-PAA diblock copolymers could still be stabilized in acid solution. Interestingly, at the intermediate pH, because of the deprotonation of P4VP (less positively charged) and protonation of PAA (less negatively charged) as well as the charge balance between the two blocks, obvious aggregation between the star-like diblock copolymer was found, representing the increased hydrodynamic size from the DLS measurements and lowered transmission in UV−vis studies. Furthermore, we note that the pH range for achieving fully stretched P4VP block and fully stretched PAA block (i.e., the solubility of the star-like diblock copolymer) may be readily tuned by different molar ratios between the two blocks. On the basis of the dual-pH responsive behavior discussed above, a class of double hydrophilic star-like diblock copolymers could be rationally designed, synthesized, and exploited as polymer nanocarriers, encapsulating different kinds of drugs that are released under varied pH ranges. For instance, drugs for oral administration should be released with increased pH while the anticancer drugs should be released at decreased pH (at tumor tissues or the endosomal and lysosomal compartments of cells).

https://dx.doi.org/10.1021/acs.macromol.0c00918
Macromolecules 2020, 53, 8286−8295

In summary, we developed an approach to prepare star-like triblock copolymers consisting of P4VP and P*t*BA as the first and second blocks with narrow MW distribution via addition of a linear initiator during the second ATRP for the polymerization of P*t*BA block. The advantages of this approach are manifested in the tailorability of the MW of each block as well as the excellent control over the MW distribution (typically lower than 1.2). The kinetics of growing the second P*t*BA block by ATRP with and without the addition of linear initiators are scrutinized. The linear relationship in both semilogarithmic kinetic plot and MW versus monomer conversion plot with the presence of linear initiators during the polymerization substantiate the suppressed termination and coupling reaction between polymer chains and the nature of living radical polymerization, respectively. The method via the deliberate introduction of linear initiators can thus resolve the coupling/termination issue during the growth of the second and third blocks with non-linear macroinitiators via ATRP, especially when pyridine-containing polymers are involved. Finally, after hydrolyzing P*t*BA block within star-like P4VP-*b*-P*t*BA diblock copolymers, the resulting star-like P4VP-*b*-PAA diblock copolymer displays an intriguing dual pH-responsive behavior, signifying its potential application as polymer nanocarriers for drug delivery. By extension, unimolecular star-like diblock or triblock copolymers composed of dissimilar stimuli-responsive blocks (e.g., pH-responsive, thermo-responsive, or photo-responsive) could also be rationally designed and synthesized via sequential ATRP from brominated cyclodextrins (i.e., α-, β-, γ-CD) as initiators. They may render a set of investigation into their appealing dual and triple stimuli-responsive properties triggered by different stimuli individually or concurrently for use in controlled delivery, sensors, nanotechnology, biotechnology, among other areas.

■ ASSOCIATED CONTENT

Supporting Information

The Supporting Information is available free of charge at https://pubs.acs.org/doi/10.1021/acs.macromol.0c00918.

Synthesizing star-like polymers as well as kinetic studies of polymerizing the second P*t*BA block with and without the addition of linear initiators, detailed information of the as-synthesized star-like polymers, influence of the amount of the linear initiator, $CuCl_2$, and the ratio of *t*BA to initiate sites on polymerization, removal of the linear initiator by washing with hexane, statistic histogram of star-like polymers measured from AFM results, FTIR of star-like P4VP-*b*-P*t*BA diblock copolymers before and after azidation, digital image of star-like P4VP homopolymers under different pH values, and changes in size (measured by DLS) and transmittance (measured by UV−vis) of star-like P4VP homopolymers and star-like PAA homopolymers under different pH environments, respectively (PDF)

■ AUTHOR INFORMATION

Corresponding Author

Zhiqun Lin − *School of Materials Science and Engineering, Georgia Institute of Technology, Atlanta, Georgia 30332, United States;* orcid.org/0000-0003-3158-9340; Email: zhiqun.lin@mse.gatech.edu

Authors

Yeu-Wei Harn − *School of Materials Science and Engineering, Georgia Institute of Technology, Atlanta, Georgia 30332, United States*

Yanjie He − *School of Materials Science and Engineering, Georgia Institute of Technology, Atlanta, Georgia 30332, United States*

Zewei Wang − *School of Materials Science and Engineering, Georgia Institute of Technology, Atlanta, Georgia 30332, United States*

Yihuang Chen − *School of Materials Science and Engineering, Georgia Institute of Technology, Atlanta, Georgia 30332, United States*

Shuang Liang − *School of Materials Science and Engineering, Georgia Institute of Technology, Atlanta, Georgia 30332, United States*

Zili Li − *School of Materials Science and Engineering, Georgia Institute of Technology, Atlanta, Georgia 30332, United States*

Qiong Li − *Department of Macromolecular Science and Engineering, Case Western Reserve University, Cleveland, Ohio 44106, United States*

Lei Zhu − *Department of Macromolecular Science and Engineering, Case Western Reserve University, Cleveland, Ohio 44106, United States;* orcid.org/0000-0001-6570-9123

Complete contact information is available at: https://pubs.acs.org/10.1021/acs.macromol.0c00918

Notes

The authors declare no competing financial interest.

■ ACKNOWLEDGMENTS

This work is supported by the Air Force Office of Scientific Research (FA9550-19-1-0317) and the National Science Foundation (DMR 1709420, Chemistry 1903957).

■ REFERENCES

(1) Matyjaszewski, K.; Tsarevsky, N. V. Nanostructured functional materials prepared by atom transfer radical polymerization. *Nat. Chem.* **2009**, *1*, 276.

(2) Bielawski, C. W.; Benitez, D.; Grubbs, R. H. An "Endless" Route to Cyclic Polymers. *Science* **2002**, *297*, 2041−2044.

(3) Pang, X.; He, Y.; Jung, J.; Lin, Z. 1D nanocrystals with precisely controlled dimensions, compositions, and architectures. *Science* **2016**, *353*, 1268−1272.

(4) Zhang, Q.; Su, L.; Collins, J.; Chen, G.; Wallis, R.; Mitchell, D. A.; Haddleton, D. M.; Becer, C. R. Dendritic cell lectin-targeting sentinel-like unimolecular glycoconjugates to release an anti-HIV drug. *J. Am. Chem. Soc.* **2014**, *136*, 4325−4332.

(5) Pang, X.; Zhao, L.; Han, W.; Xin, X.; Lin, Z. A general and robust strategy for the synthesis of nearly monodisperse colloidal nanocrystals. *Nat. Nanotechnol.* **2013**, *8*, 426.

(6) Li, F.; Cao, M.; Feng, Y.; Liang, R.; Fu, X.; Zhong, M. Site-Specifically Initiated Controlled/Living Branching Radical Polymerization: A Synthetic Route toward Hierarchically Branched Architectures. *J. Am. Chem. Soc.* **2018**, *141*, 794−799.

(7) Zhao, Y.; Shuai, X.; Chen, C.; Xi, F. Synthesis of star block copolymers from dendrimer initiators by combining ring-opening polymerization and atom transfer radical polymerization. *Macromolecules* **2004**, *37*, 8854−8862.

(8) Daniel, W. F. M.; Burdyńska, J.; Vatankhah-Varnoosfaderani, M.; Matyjaszewski, K.; Paturej, J.; Rubinstein, M.; Dobrynin, A. V.; Sheiko, S. S. Solvent-free, supersoft and superelastic bottlebrush melts and networks. *Nat. Mater.* **2016**, *15*, 183.

(9) Chen, Y.; Yang, D.; Yoon, Y. J.; Pang, X.; Wang, Z.; Jung, J.; He, Y.; Harn, Y. W.; He, M.; Zhang, S.; Zhang, G.; Lin, Z. Hairy uniform permanently ligated hollow nanoparticles with precise dimension

control and tunable optical properties. *J. Am. Chem. Soc.* **2017**, *139*, 12956−12967.
(10) He, Y.; Pang, X.; Jiang, B.; Feng, C.; Harn, Y.-W.; Chen, Y.; Yoon, Y. J.; Pan, S.; Lu, C.-H.; Chang, Y.; Zebarjadi, M.; Kang, Z.; Thadhani, N.; Peng, J.; Lin, Z. Unconventional Route to Uniform Hollow Semiconducting Nanoparticles with Tailorable Dimensions, Compositions, Surface Chemistry, and Near-Infrared Absorption. *Angew. Chem.* **2017**, *129*, 13126−13131.
(11) Li, S.; Mohamed, A. I.; Pande, V.; Wang, H.; Cuthbert, J.; Pan, X.; He, H.; Wang, Z.; Viswanathan, V.; Whitacre, J. F.; Matyjaszewski, K. Single-ion homopolymer electrolytes with high transference number prepared by click chemistry and photoinduced metal-free atom-transfer radical polymerization. *ACS Energy Lett.* **2017**, *3*, 20−27.
(12) Koda, Y.; Terashima, T.; Nomura, A.; Ouchi, M.; Sawamoto, M. Fluorinated microgel-core star polymers as fluorous compartments for molecular recognition. *Macromolecules* **2011**, *44*, 4574−4578.
(13) Terashima, T.; Kamigaito, M.; Baek, K.-Y.; Ando, T.; Sawamoto, M. Polymer catalysts from polymerization catalysts: direct encapsulation of metal catalyst into star polymer core during metal-catalyzed living radical polymerization. *J. Am. Chem. Soc.* **2003**, *125*, 5288−5289.
(14) Du, H.; Han, R.; Tang, E.; Zhou, J.; Liu, S.; Guo, X.; Wang, R. Synthesis of pH-responsive cellulose-g-P4VP by atom transfer radical polymerization in ionic liquid, loading, and controlled release of aspirin. *J. Polym. Res.* **2018**, *25*, 205.
(15) Matyjaszewski, K.; Miller, P. J.; Pyun, J.; Kickelbick, G.; Diamanti, S. Synthesis and characterization of star polymers with varying arm number, length, and composition from organic and hybrid inorganic/organic multifunctional initiators. *Macromolecules* **1999**, *32*, 6526−6535.
(16) Mayadunne, R. T. A.; Jeffery, J.; Moad, G.; Rizzardo, E. Living Free Radical Polymerization with Reversible Addition−Fragmentation Chain Transfer (RAFT Polymerization): Approaches to Star Polymers. *Macromolecules* **2003**, *36*, 1505−1513.
(17) Matyjaszewski, K.; Patten, T. E.; Xia, J. Controlled/"living" radical polymerization. Kinetics of the homogeneous atom transfer radical polymerization of styrene. *J. Am. Chem. Soc.* **1997**, *119*, 674−680.
(18) Angot, S.; Murthy, K. S.; Taton, D.; Gnanou, Y. Scope of the Copper Halide/Bipyridyl System Associated with Calixarene-Based Multihalides for the Synthesis of Well-Defined Polystyrene and Poly(meth)acrylate Stars. *Macromolecules* **2000**, *33*, 7261−7274.
(19) Cheng, G.; Böker, A.; Zhang, M.; Krausch, G.; Müller, A. H. E. Amphiphilic Cylindrical Core−Shell Brushes via a ″Grafting From″ Process Using ATRP. *Macromolecules* **2001**, *34*, 6883−6888.
(20) Yin, M.-J.; Yao, M.; Gao, S.; Zhang, A. P.; Tam, H.-Y.; Wai, P.-K. A. Rapid 3D Patterning of Poly(acrylic acid) Ionic Hydrogel for Miniature pH Sensors. *Adv. Mater.* **2016**, *28*, 1394−1399.
(21) Xiong, D. a.; He, Z.; An, Y.; Li, Z.; Wang, H.; Chen, X.; Shi, L. Temperature-responsive multilayered micelles formed from the complexation of PNIPAM-b-P4VP block-copolymer and PS-b-PAA core-shell micelles. *Polymer* **2008**, *49*, 2548−2552.
(22) Li, D.; He, Q.; Cui, Y.; Li, J. Fabrication of pH-Responsive Nanocomposites of Gold Nanoparticles/Poly(4-vinylpyridine). *Chem. Mater.* **2007**, *19*, 412−417.
(23) Pang, X.; Zhao, L.; Feng, C.; Lin, Z. Novel Amphiphilic Multiarm, Starlike Coil-Rod Diblock Copolymers via a Combination of Click Chemistry with Living Polymerization. *Macromolecules* **2011**, *44*, 7176−7183.
(24) Yang, R.; Wang, Y.; Wang, X.; He, W.; Pan, C. Synthesis of poly(4-vinylpyridine) and block copoly (4-vinylpyridine-b-styrene) by atom transfer radical polymerization using 5,5,7,12,12,14-hexamethyl-1,4,8,11-tetraazamacrocyclotetradecane as ligand. *Eur. Polym. J.* **2003**, *39*, 2029−2033.
(25) Liu, T.; Casado-Portilla, R.; Belmont, J.; Matyjaszewski, K. ATRP of butyl acrylates from functionalized carbon black surfaces. *J. Polym. Sci. Part A: Polym. Chem.* **2005**, *43*, 4695−4709.
(26) Couet, J.; Biesalski, M. Surface-Initiated ATRP ofN-Isopropylacrylamide from Initiator-Modified Self-Assembled Peptide Nanotubes. *Macromolecules* **2006**, *39*, 7258−7268.
(27) Ejaz, M.; Ohno, K.; Tsujii, Y.; Fukuda, T. Controlled grafting of a well-defined glycopolymer on a solid surface by surface-initiated atom transfer radical polymerization. *Macromolecules* **2000**, *33*, 2870−2874.
(28) Cheng, N.; Azzaroni, O.; Moya, S.; Huck, W. T. S. The effect of [CuI]/[CuII] ratio on the kinetics and conformation of polyelectrolyte brushes by atom transfer radical polymerization. *Macromol. Rapid Commun.* **2006**, *27*, 1632−1636.
(29) Kreutzer, G.; Ternat, C.; Nguyen, T. Q.; Plummer, C. J. G.; Månson, J.-A. E.; Castelletto, V.; Hamley, I. W.; Sun, F.; Sheiko, S. S.; Herrmann, A.; Ouali, L.; Sommer, H.; Fieber, W.; Velazco, M. I.; Klok, H.-A. Water-soluble, unimolecular containers based on amphiphilic multiarm star block copolymers. *Macromolecules* **2006**, *39*, 4507−4516.
(30) Houbenov, N.; Minko, S.; Stamm, M. Mixed polyelectrolyte brush from oppositely charged polymers for switching of surface charge and composition in aqueous environment. *Macromolecules* **2003**, *36*, 5897−5901.
(31) Iatridi, Z.; Tsitsilianis, C. pH responsive MWCNT-star terpolymer nanohybrids. *Soft Matter* **2013**, *9*, 185−193.

https://dx.doi.org/10.1021/acs.macromol.0c00918
Macromolecules 2020, 53, 8286−8295